Korean J Physiol Pharmacol 2018;22(3):291-300
https://doi.org/10.4196/kjpp.2018.22.3.291

KJPP

Original Article

Establishment and evaluation of the VX2 orthotopic lung cancer rabbit model: a ultra-minimal invasive percutaneous puncture inoculation method

Lijuan Wang[1,2], Keke Che[3], Zhonghong Liu[2], Xianlong Huang[4], Shifeng Xiang[4], Fei Zhu[2], and Yu Yu[2,*]

[1]*Department of Pharmacy, Chongqing Engineering Research Center of Pharmaceutical Sciences, Chongqing Medical and Pharmaceutical College, Chongqing 401331,* [2]*Pharmacy College, Chongqing Medical University, Chongqing 400016,* [3]*Department of Pharmacy, Chongqing General Hospital, Chongqing 400014,* [4]*Radiology Department, Chongqing General Hospital, Chongqing 400014, China*

ARTICLE INFO

Received September 5, 2017
Revised January 2, 2018
Accepted January 27, 2018

***Correspondence**
Yu Yu
E-mail: yuyu3519@163.com

Key Words
Fast method
Minimal invasive
Percutaneous puncture inoculation
VX2 orthotopic lung cancer rabbit model

ABSTRACT The purpose of the present work is to establish an ultra-minimal invasive percutaneous puncture inoculation method for a VX2 orthotopic lung cancer rabbit model with fewer technical difficulties, lower mortality of rabbits, a higher success rate and a shorter operation time, to evaluate the growth, metastasis and apoptosis of tumor by CT scans, necropsy, histological examination, flow cytometry and immunohistochemistry. The average inoculation time was 10-15 min per rabbit. The tumor-bearing rate was 100%. More than 90% of the tumor-bearing rabbits showed local solitary tumor with 2-10 mm diameters after two weeks post-inoculation, and the rate of chest seeding was only 8.3% (2/24). The tumors diameters increased to 4-16 mm, and irregularly short thorns were observed 3 weeks after inoculation. Five weeks post-inoculation, the liquefaction necrosis and a cavity developed, and the size of tumor grew further. Before natural death, the CT images showed that the tumors spread to the chest. The flow cytometry and immunohistochemistry indicated that there was less apoptosis in VX2 orthotopic lung cancer rabbit model compared to chemotherapy drug treatment group. Minimal invasive percutaneous puncture inoculation is an easy, fast and accurate method to establish the VX2 orthotopic lung cancer rabbit model, an ideal *in situ* tumor model similar to human malignant tumor growth.

INTRODUCTION

Lung cancer incidence and mortality have been increasing in many parts of the world, making lung cancer a major and serious public health problem [1-3]. In 2012, approximately 1.8 million new cases of lung cancer were diagnosed and 1.6 million patients died of lung cancer. Although surgical resection applies to early-stage lung cancer, most primary and secondary lung cancer patients require chemotherapy and radiation. Unfortunately, long-term survival remains poor. Local targeting drug delivery systems to target intrapulmonary tumors have been developed to reduce systemic side effects and improve the curative effect [4-6]. To evaluate the antitumor effect of these preparations, it is necessary to establish a lung cancer animal model.

Currently, tumor-bearing nude/immunodeficient mouse model of lung cancer has been extensively applied for pharmacodynamics studies due to its convenience in establishment and in the observation of tumor growth. These lung cancer models have been constructed with human tumor cells suspension, such as A549 cells, through ectopic subcutaneous injection [7,8] or endobronchial/intrapulmonary injection [9-11]. Nonetheless, the tumor-bearing mouse model does not completely represent the actual circumstance of tumor cell growth since the implantation are allografts. Mouse xenografts that grow in an environment that is highly

Author contributions: L.J.W. and K.K.C. performed all experiments and contributed equally to this work. L.H.Z. and F.Z. participated the animal experiment. X.L.H. and S.F.X. analyzed the CT images. L.J.W. drafted the manuscript. Y.Y. conceived the project and revised the manuscript.

dissimilar to that of their originating tumor frequently result in promising treatments that are ultimately clinically ineffective.

The VX2 lung cancer rabbit model has been currently in use due to its orthotopic growth and the homograft of tumor. It is a more ideal lung cancer model to simulate growth and metastasis of tumor in vivo. The VX2 tumor is a virus-induced papilloma of rabbits which could be implanted within the tissues and caused protuberances [12,13]. VX2 tumor-bearing model is a big tumor model and closely imitates human lung cancer initiation, development and progress [14]. Previous methods reported for the establishment of the VX2 lung cancer rabbit model include the percutaneous injection of VX2 tumor cells suspension with/without computed tomography (CT) [15,16] and implantation of VX2 tumor tissue fragments under traditional thoracotomy [17,18]. However, the former method utilizes tumor cells suspension, which may result in pleural dissemination and multifocal growth. The latter method can easily cause pneumothorax and a longer operation time, which requires the experiment operator to have considerable proficiency or surgical operation experience.

Due to certain limitations of the two kind of methods, the purpose of the present work is to establish an ultra-minimal invasive orthotopic VX2 homograft model in rabbits with fewer technical difficulties, lower mortality of rabbits, a higher success rate and a shorter operation time. We evaluated the tumor growth, metastasis and apoptosis of tumor by CT scans, necropsy, histological examination, flow cytometry and immunohistochemistry.

METHODS

Animals and animal care

Twenty-four New Zealand white rabbits (Chongqing Medical University), male or female, weighting between 2.0 and 3.0 kg, were used and allowed free access to food and water before inoculation. The rabbits were housed in individual steel cages under the following conditions: 12 h light-dark cycle with an environmental temperature maintained at 18-26°C as approved by the laboratory animal center of Chongqing Medical University. Approval of the experimental protocol was obtained from the Animal Experiments Committee of Chongqing Medical University to ensure the humane treatment of test animals.

VX2 tumor fragments

VX2 tumor tissues obtained from the Biomedical Engineering Institute of Chongqing Medical University were stored in 0.9% NaCl injection at 4°C. The regions near the rim of tumor tissues, which contained less necrotic tissue, were cut into small fragments (approximately 1.0 mm^3). A VX2 tumor fragment was drawn into an 18-gauge needle (Shanghai Puyi Medical Instruments Co., Ltd) with two pieces of absorbable gelatin sponge (approximately 0.5 cm) placed in front and back of it.

Percutaneous puncture inoculation

The VX2 orthotopic lung cancer rabbit model was established by minimally invasive percutaneous puncture inoculation. Rabbits used for inoculation were anesthetized by an intravenous injection of pentobarbital sodium (3%, 1 ml/kg, ourchem®, shanghai) and fixed on the digital gastrointestinal machine (UD150L-30E, Shimadzu) (Fig. 1A). The right chest regions were shaved and disinfected. The percutaneous puncture inoculation of VX2 tumor fragments was divided into two steps: (1) The 18-gauge needle with VX2 tumor fragments and gelatin sponge was placed on the right chest region of a rabbit in vitro. The point, angle and depth of puncture were determined under the image guidance of the digital gastrointestinal machine (Fig. 1B). (2) The

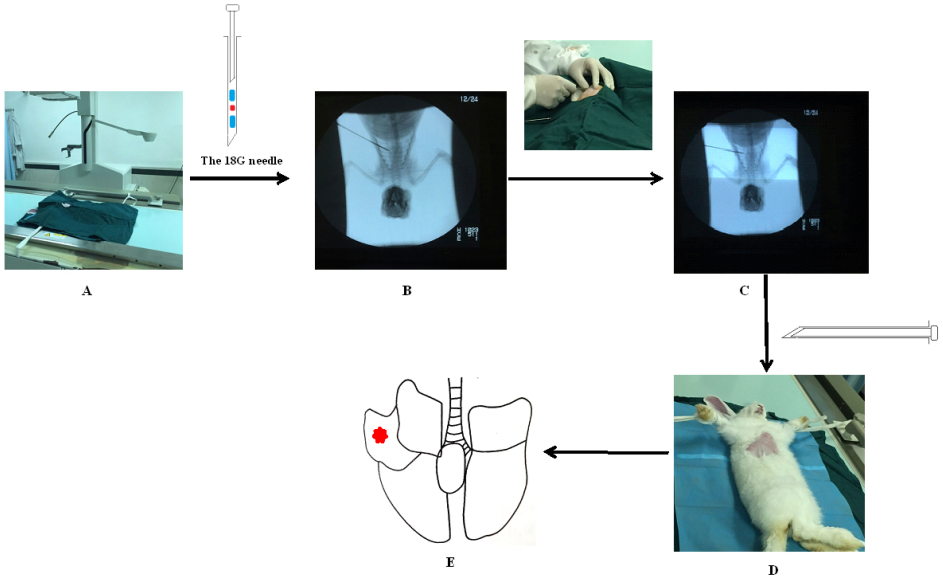

Fig. 1. The procedure of minimal invasive percutaneous puncture inoculation to establish VX2 orthotopic lung cancer rabbits model. (A) Rabbit was fixed on the digital gastrointestinal machine (and 18-gauge needle was prepared before inoculation. Blue: 0.5 cm gelatin sponge, red: 1 mm^3 tumor fragment); (B) Step 1: position in vitro; (C) Step 2: position in vivo; (D) Withdrawing the needle; (E) The probable position of tumors (confirmed by Fig. 2).

rabbit received percutaneous puncture though the right chest by the 18-gauge needle. The position of the gauge needle in vivo was determined under the image guidance of the digital gastrointestinal machine secondly (Fig. 1C). When the needle point was inserted into the right lung of rabbit, the VX2 tumor fragments and the gelatin sponge were pushed into the right lung together. Finally, after withdrawing the needle, pressure was applied to the puncture point for 90 seconds (Fig. 1D). After the inoculation, an intramuscular injection of cefradine (0.25 g/day, North China Pharmaceutical group co., Ltd) was given to each rabbit to prevent infection.

Experimental group

The rabbits that received percutaneous puncture inoculation for two weeks were randomly divided into four groups: Group A (received CT scans to nature death, n=6), Group B (sacrificed at three weeks post-inoculation, n=6), Group C (sacrificed at five weeks post-inoculation, n=6), and Group D (positive control, received chemotherapy drug docetaxel, n=6).

CT scanning

Six rabbits in Group A were subjected to CT scans (Aquilion CXL, TOSHIBA) at 2, 3, 5, 7 and 9 week post-inoculation. The rabbits were anesthetized by intravenous injection of pentobarbital sodium (3%, 0.5 ml/kg) before CT scanning. The scan parameters were 80 Kv, 30 mA, 5 mm slice thickness, pulmonary window: 1200 HU window width, –400 HU window level, mediastinal window: 300 HU window width, 25 HU window level. Tumor length, width and thickness were determined to calculate the tumor volume according to the following formula:

$$V\ (mm^3)=L\ (mm)\times S^2\ (mm^2)/2$$

V: Tumor volume. L: Largest diameter (the maximum value of tumor length, width and thickness). S: Smallest diameter (the minimum value of tumor length, width and thickness).

The double time (DT) of the tumor was calculated according to the following formula:

$$DT=\frac{lg2\times\Delta t}{lg\left(\frac{V2}{V1}\right)}$$

Δt: time interval (days) of two successive CT scans; V2: the latter tumor volume of two successive CT scans; V1: the previous tumor volume of two successive CT scans.

Necropsy and tissue preparation

Six rabbits in group A were sacrificed after natural death and the daily behavior, such as weight and breathing, were recorded during survival time. Twelve rabbits in group B and C were sacrificed by an intravenous injection of pentobarbital sodium (3%, 1.5-2.0 ml/kg) at 3 or 5 weeks. All 18 animals were dissected after sacrifice or natural death. The lungs, pleural cavity, mediastinum, heart, liver, kidney and spleen were examined for evidence of tumor growth and metastasis. For the hemotoxylin and eosin (HE) staining procedures and the immunohistochemical analysis, one part of the tumor was fixed in formalin and embedded in paraffin. Another part of the tumor was washed in cold PBS for flow cytometry.

Immunohistochemistry by TUNEL and CD31 assay

Tumor apoptosis was measured using a TUNEL assay. Tumor

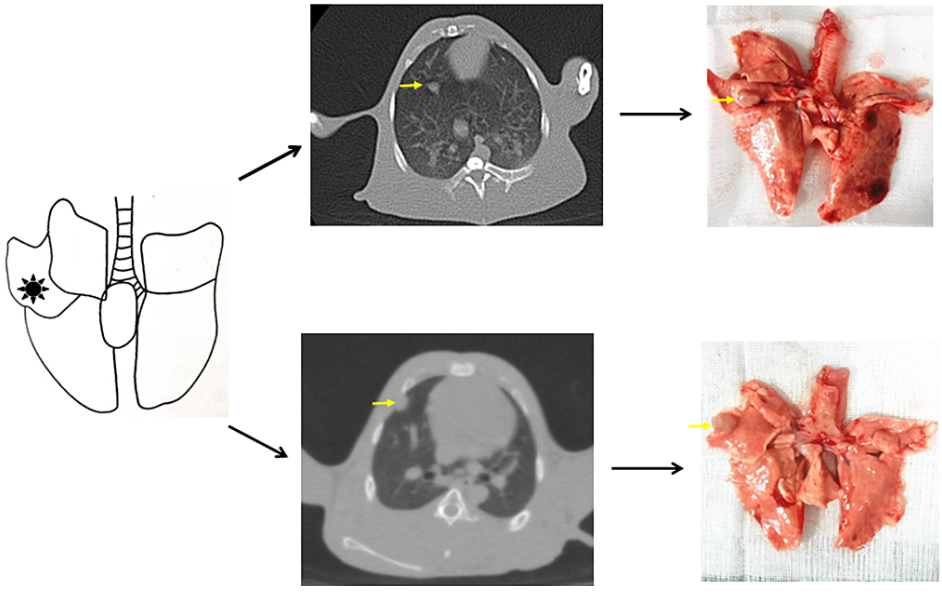

Fig. 2. The probable position of tumors confirmed by CT scanning and necropsy.

angiogenesis was measured with immunohistochemistry by a CD31 assay. The paraffin sections (5 μm) were dewaxed with xylene and a gradient concentration of ethanol. Then, they were washed with PBS (pH7.2-7.4, Beijing Jinshan biotechnology co., Ltd) three times. The sections were incubated in 3% H_2O_2 and proteinase K (Merck Millipore) and reacted with a TUNEL (in situ cell death detection kit-POD method, Roche Group) mixture for 1 h. After washing with PBS, the sections were incubated with streptavidin-HRP (1:400) for 30 min at 37°C and rewashed with PBS. Then the sections were incubated with DAB solution (Beijing Jinshan biotechnology co., Ltd) for 10 min. Finally, counterstaining was performed with hematoxylin (Beijing Jinshan biotechnology co., Ltd). Afterwards, the tumor slides were imaged under a microscope. The apoptosis rate was quantified as the percent of TUNEL-positive cells relative to the total number of cells. The procedure of the CD31 assay was performed as previously described with minor modifications. Briefly, mouse anti-CD31 monoclonal antibody (Immunoway®) was incubated as the primary antibody. The CD31-positive cells were observed under a microscope.

Flow cytometry

The tumors washed by cold PBS were cut into 0.1 mm^3 pieces to release of the tumor cells. Next, the tumor pieces were sifted by a 200-mesh cell strainer to remove the cell mass and debris. The cell suspensions after sifting were centrifuged at 1000 rpm and resuspended in cold PBS. The tumor cells were stained with annexin V-FITC and PI. Flow cytometry performed to analyze apoptosis according to the manufacturer's instructions (FACScan Becton Dickinson). Approximately 10^4 events (cells) were evaluated for each sample.

Positive control

Six rabbits from group D were intravenously injected with docetaxel (Taxotere®, Aventis Pharma) for three weeks (1 mg/kg, once a week) after 2 weeks post-inoculation as positive control. Docetaxel was a chemotherapy drug that has been proven to promote tumor apoptosis. We compared the apoptosis of the group C and D to indicate the growth state of the tumor in VX2 orthotopic lung cancer rabbit model. The rabbits were sacrificed by intravenous injection of pentobarbital sodium (3%, 1.5-2.0 ml/kg) after the last administration. The tumor tissues were prepared for immunohistochemical analysis and flow cytometry as described above.

Statistical analysis

The statistical analysis was performed with SPSS 23.0 software (IBM®). The tumor growth curve was generated using the volume data from localized intrapulmonary tumors in the CT scanning images. The statistical significances of differences in tumor

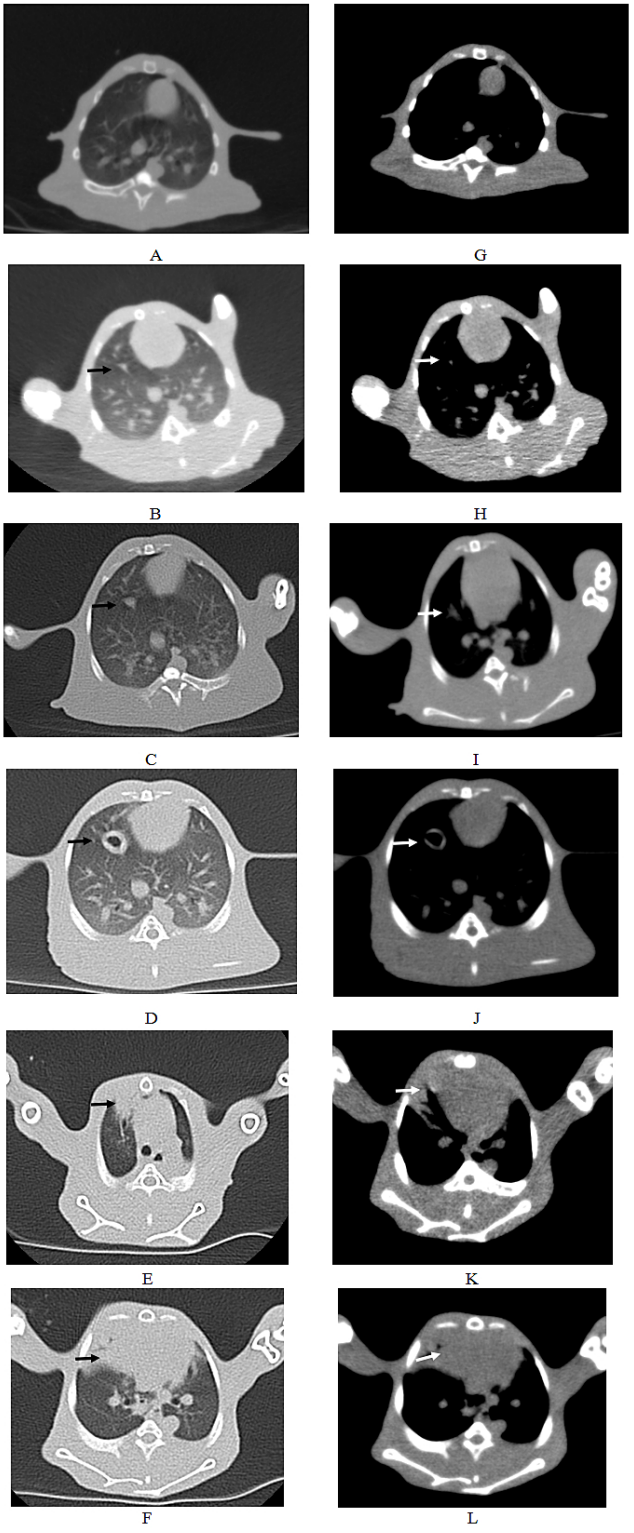

Fig. 3. CT scanning images of rabbit with the longest survival time (CT2). (A-F) Pulmonary window. The black arrows indicated the intrapulmonary tumors; (G-L) Mediastinal window. The white arrows indicated the intrapulmonary tumors; The other white spots represented the blood vessels in the lung. (A, G) There were no tumors in the right lung before inoculation. (B, H) 2 weeks post inoculation. (C, I) 3 weeks post inoculation. (D, J) 5 weeks post inoculation. (E, K) 7 weeks post inoculation. (F, L) 9 weeks post inoculation.

growth and apoptosis were calculated using the unpaired Student's *t*-test. A p value less than 0.05 was considered significant.

RESULTS

CT scanning

Solitary and localized intrapulmonary tumors were discovered in the six rabbits that received CT scans. Fig. 2 shows the probable position of the tumors using percutaneous puncture inoculation under the image guidance of the digital gastrointestinal machine. Tab. 1 shows the results of CT scans including tumor size, shape and metastasis (n=6) at 2, 3, 5, 7 and 9 weeks post-inoculation. Fig. 3 shows the CT scanning images of the rabbit with the longest survival time (CT2). Two weeks post-inoculation, the single and localized intrapulmonary tumors with 2-10 mm diameters showed growth as ellipsoidal or irregularly circular nodes. The tumors increased to 4-16 mm in diameter and irregularly short thorns were seen in the pulmonary window after 3 weeks of inoculation. Five weeks post-inoculation, the liquefaction necrosis and the cavity were formed in the tumors, with the size of tumor increasing further (6-16 mm). Over the next few weeks, the tumors with more thorns began to spread in the right lung. Before natural death, the CT image showed that the tumors had spread to the chest and the boundary with the heart was not clear.

The length, width and thickness of the tumors were evaluated and recorded by experienced radiologists according to the CT image, then the volumes were calculated. The tumor growth curve is shown in Fig. 4 (Mean±SD). The DTs of the tumors were 3.5 d, 7.3 d and 18.1 d during 2 to 3 weeks, 3 to 5 weeks, 5 to 7 weeks, respectively.

Necropsy and histology

Rabbits from group B and C were sacrificed at 3 weeks (n=6) or 5 weeks (n=6). Solitary tumors were found in the former rabbits (Fig. 5A, n=5) one rabbit had confirmed chest seeding (Fig. 5B, n=1). The solitary tumors with liquefaction necrosis and cavities were found in the latter rabbits (Fig. 5E, n=4); with two rabbits that showed solitary tumors and pleural metastases (Fig. 5F, n=2); and one rabbit with confirmed chest seeding (n=1). The tumors were checked by HE staining (Figs. 5C, D, G, H) to reveal the degree of necrosis and tumor cell shapes. Tumor-bearing rabbits showed large nests with distinct cell borders. Less necrosis and more pleomorphic nuclei were observed. Five weeks after incubation, the tumors spread in the right lung and showed pleural metastases. A large number of acidophilic leukocytes and macro-

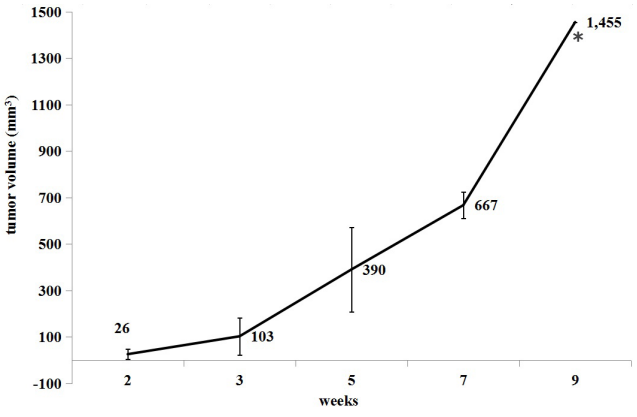

Fig. 4. Growth curve of tumor 2-9 weeks post-inoculation (Mean± SD). *At nine weeks post-inoculation, there was no SD value due to death of rabbit.

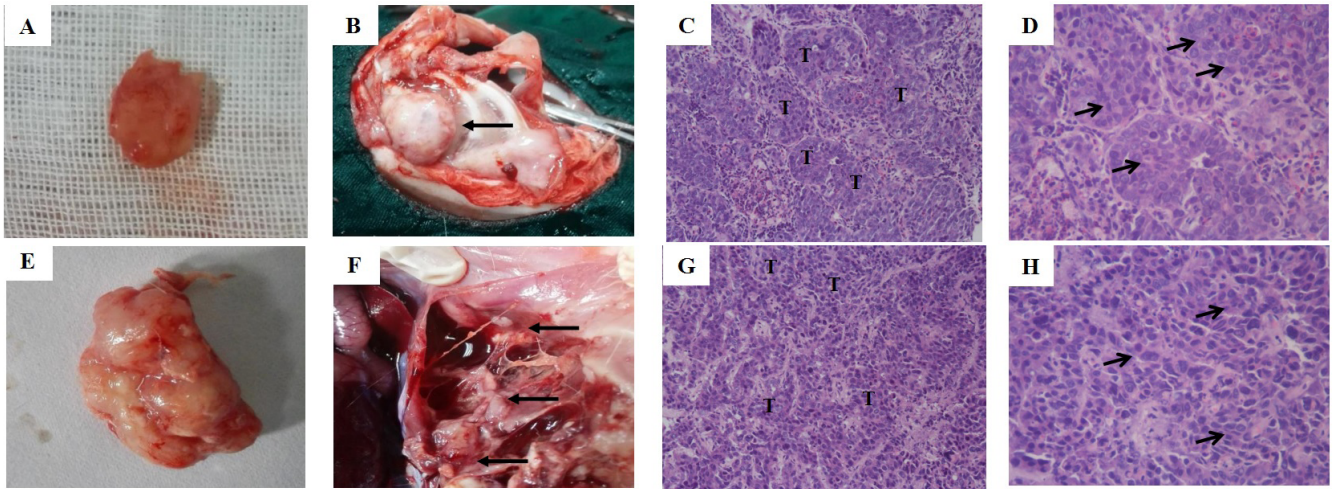

Fig. 5. Necropsy and histological findings. (A) The photograph of solitary tumor at 3 weeks post-incubation. (B) The chest seeding (black arrows); (C, D) The histological view of tumor at 3 weeks post-incubation (C: 20×; D: 40×); (E) The photograph of solitary tumor with liquefaction necrosis and cavity at 5 weeks post-incubation; (F) Pleural metastases (black arrows); (G-H) The histological view of tumor at 5 weeks post-incubation (C: 20×; D: 40×). "T" shows tumor, black arrows show tumor cells.

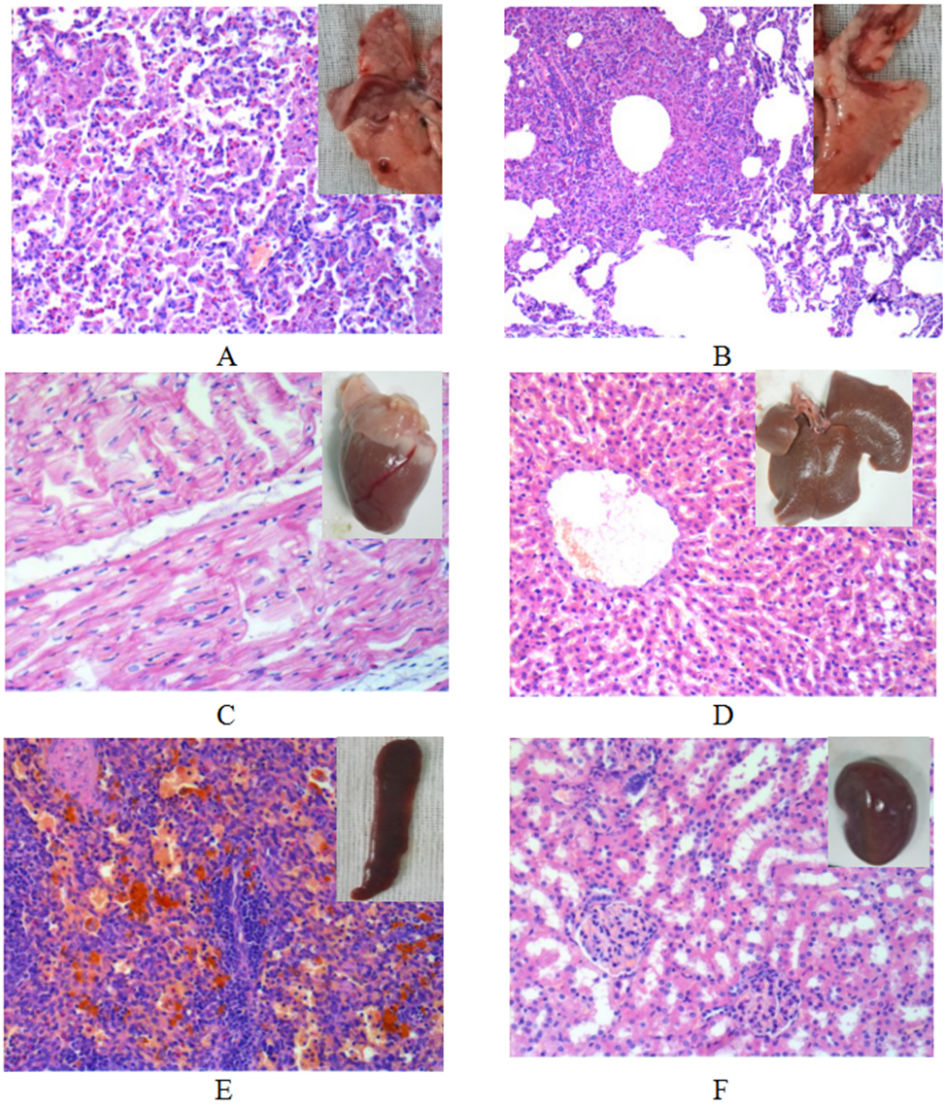

Fig. 6. The histological view of tissues except tumor (20×). (A) Right lung; (B) left lung; (C) heart; (D) liver; (E) spleen; (F) kidney.

phages were visible with distortion of the right lung architecture (Fig. 6A). No left lung, liver, spleen, heart or kidney metastases were observed in any of the rabbits in either necropsy or histological sections (Figs. 6B-F).

Survival situation

Six rabbits that received CT scans all died of respiratory failure. The survival times are shown in Table 1. The body weights and the general status of the tumor-bearing rabbits during survival time were recorded. During the first three weeks after incubation, the tumor-bearing rabbits showed normal in breathing and activities without diarrhea or molt. During the fourth and fifth weeks, the tumor-bearing rabbits showed reduced food intake and lower body weights and activities. Some tumor-bearing rabbits had difficulty breathing. After five weeks, some tumor-bearing rabbits died a natural death via respiratory failure. Before the death, a sharp drop in weight was observed. The weight change curve is shown in Fig. 7A. The mean value of survival time was 42.2d (Fig. 7B).

Apoptosis of tumor

The apoptosis of tumor tissues in group C and D was confirmed by flow cytometry (Fig. 8A) and TUNEL assay (Fig. 8B). The total apoptosis rate resulted from flow cytometry in group C and group D were 28.71±5.06% and 43.40±2.26%, respectively. The total apoptosis rate in group D was significantly higher than in the group C ($p<0.01$). The number of TUNEL-positive cells, which represent apoptotic tumor cells, in group D was significantly higher than in the group C ($p<0.01$). The total apoptosis rates resulted from TUNEL test in group C and group D were 8.4±0.9% and 12.2±1.1%, respectively. CD31 was used to evaluate the degree of tumor angiogenesis, which indicates a rapidly growing tumor. Group C had stronger CD31 immunostaining than group D, suggesting that the tumor in the VX2 orthotopic rabbit model grew well and was inhibited after drug treatment (Fig. 8C).

Table 1. Results of CT Scanning and survival (2, 3, 5, 7 and 9 weeks after inoculation)

Week	2			3			5			7			9			Survival time	Cause of death
No.*	T# (mm)	CS**	ME##	T (mm)	CS	ME	T (mm)	CS	ME	T (mm)	CS	ME	T (mm)	CS	ME		
CT1	5.1×3.7×9.0	No	No	7.4×5.5×11.5	No	Yes	12.1×8.5×14.0	No	Yes	***	***	***	***	***	***	30	RF
CT2	2.2×2.1×3.5	No	No	5.1×3.3×6.5	No	No	8.9×5.4×10.5	No	No	11.6×9.4×16.0	No	Yes	12.0×11.5×22.0	No	Yes	57	RF
CT3	5.2×2.8×7.5	No	No	9.5×6.1×10.5	No	No	11.5×9.0×12.5	No	Yes	***	***	***	***	***	***	34	RF
CT4	4.9×4.6×4.0	No	No	8.3×5.2×11.5	No	No	9.0×7.6×16.5	No	Yes	***	***	***	***	***	***	36	RF
CT5	2.9×2.3×4.0	No	No	5.0×3.5×7.0	No	No	10.2×9.1×13.0	No	Yes	***	***	***	***	***	***	42	RF
CT6	2.2×1.8×3.5	No	No	4.3×2.4×4.5	No	No	6.3×5.3×11.5	No	No	9.6×9.3×14.5	No	Yes	***	***	***	54	RF

*CT1 means the first rabbit for CT scanning. #T means the tumor length, width and thickness. **CS means chest seeding. ##Means pleural or mediastinal metastasis. RF means respiratory failure. ***Death.

DISCUSSION

The VX2 lung cancer rabbit model is an ideal lung cancer model to evaluate the antitumor effects of lung tumor-targeted formulations in vivo due to its orthotopic, aggressive and metastatic growth. However, the previous methods reported for the establishment of the VX2 lung cancer rabbit model have several disadvantages including pleural dissemination, multifocal growth and pneumothorax. Few studies could establish the VX2 lung cancer rabbit model quickly, massively and accurately. Most of the experiment operators were surgeons or had considerable proficiency or surgical operation experience.

In our study of the minimal invasive percutaneous puncture inoculation, we inoculated eight lung cancer models with implantation of the VX2 tumor tissue fragments under traditional thoracotomy. However, five rabbits of them died of pneumothorax during the inoculation, with a mortality rate of up to 62.5% (5/8). The minimal invasive percutaneous puncture inoculation method to establish VX2 orthotopic lung cancer rabbits model in our study overcame the limitations of the previous methods with less technical difficulties, decreased mortality of the rabbits and a higher success rate. All the tumor-bearing rabbits with our method survived and the mortality rate was 0% (0/24). More importantly, it provided an operable and practical method for ordinary researchers. It is an easy, fast and accurate method to establish the VX2 orthotopic lung cancer rabbit model through two-perspective positioning in vivo and in vitro. The average inoculation time was 10-15 min per rabbit and the incubation of the 24 rabbits finished within 8 hours. The tumor bearing rate was 100%. More than 90% of the tumor-bearing rabbits showed local solitary tumors and the rate of chest seeding was only 8.3% (2/24). The minimal invasive percutaneous puncture inoculation method to establish VX2 orthotopic lung cancer rabbit model is faster and more effective than previous methods [15-17].

To ensure the success rate of incubation, it is necessary to pay attention to the following elements during the minimal invasive percutaneous puncture process: (1) The selection of tumor fragments. The regions near the rim of the tumor, which contained less necrotic tissue, should be selected. Tumor fragments should not to be too large (1 mm^3). (2) The biodegradable collagen should be placed in front of and behind the tumor fragment in the 18G needle to prevent the escape of tumor fragments along the puncture, which leads to chest seeding. (3) The incubation process should be as fast as possible to avoid repeat punctures, which leads to pneumothorax. (4) The position of the gauge needle in vitro and vivo was determined under the image guidance of a digital gastrointestinal machine. According to our experience, the superior puncture position is between the fourth and fifth rib to avoid large blood vessels. The depth of the puncture position is approximately 1 cm. (5) Use antibiotics as necessary to avoid infection after percutaneous puncture.

Currently, VX2 transplantation tumor rabbit models of differ-

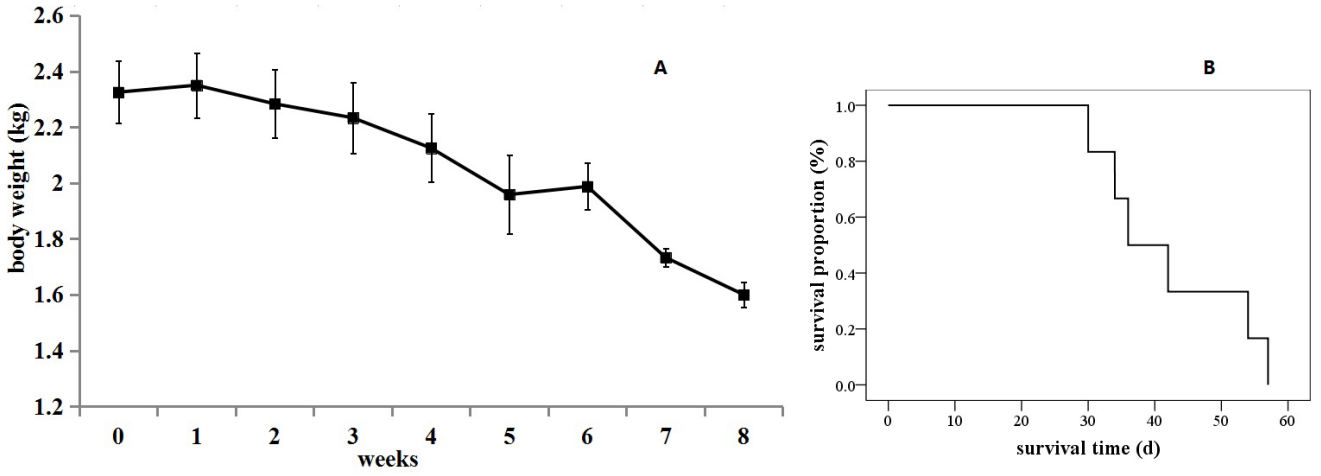

Fig. 7. The survival situation of the VX2 orthotopic lung cancer rabbits. (A) The curve of body weight change. Results are means±SD, n=6. (B) Kaplan-Meier survival curves (n=6).

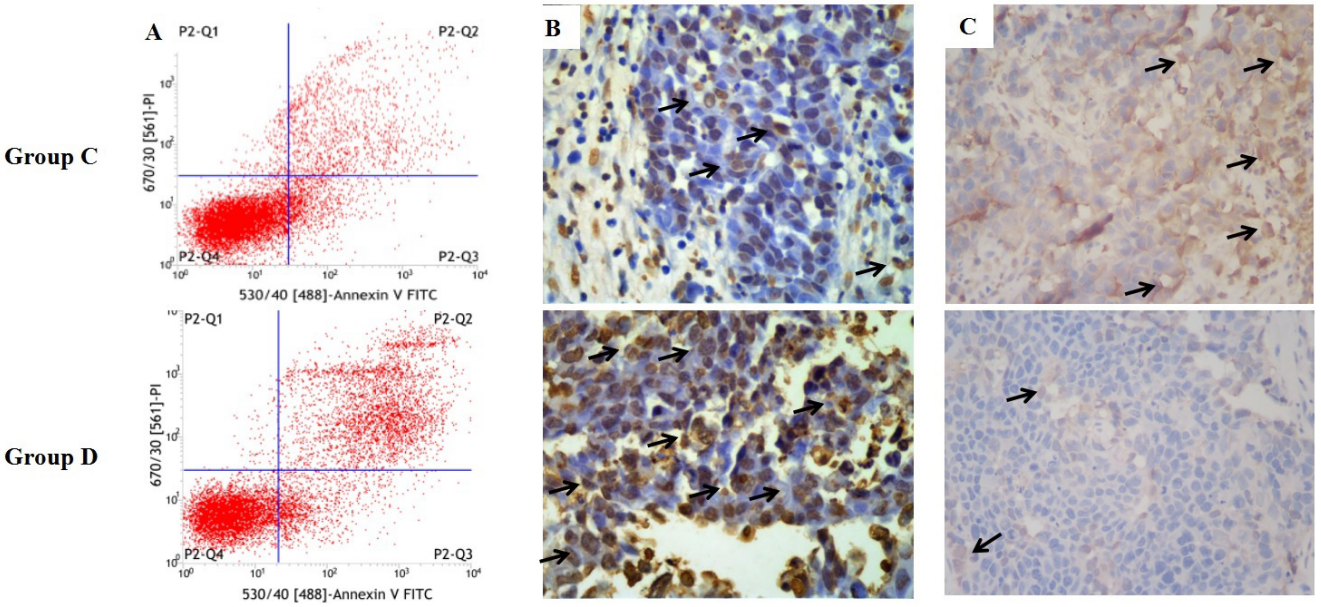

Fig. 8. The apoptosis of VX2 orthotopic lung cancer rabbit model in group C and D. (A) Flow cytometry; (B) Immunohistochemistry by TUNEL assay (brown cells means TUNEL-positive cells which indicates tumor apoptosis); (C) Immunohistochemistry by CD31 assay (brown means CD31-positive which indicate tumor angiogenesis).

ent organs are widely used [19-22]. When the VX2 tumor cells or fragments were transplanted into the lungs of rabbits, they glew rapidly and invaded nearby lung tissues. The CT images demonstrated three phases of the intrapulmonary tumor growth: tumor blood vessel formation phase, blood vessel stabilization phase and blood vessel degradation phase [23-25]. In weeks 2 to 3, the tumors were solitary nodes within formation of many blood capillaries, provided nutrition for tumor growth. Less necrosis was evident during this phase. In the third or fourth week, the volumes of the tumors were glew more quickly than tumor blood vessels. The center of the tumor showed necrosis due to ischemia. This phase was called the blood vessel stabilization phase. Then, some tumors showed invasion of the pleura and the rabbits suffered poor mental states, emaciation and gasping. In the blood vessel degradation phase, tumor necrosis was increased and atelectasis of right lung was also observed on CT images. Meanwhile the rabbits showed breathing difficulty and even died of respiratory failure. To ensure that tumor growth is similar, it is important to use VX2 tumor fragments of the same source. The appropriate time to use the model to the evaluate effects of antitumor drugs or novel formulations is around the second and third week.

Tumor double time (DT), an indicator of benign and malignant identification, represents the time required for the tumor volume or the tumor cell number to double. In our study, the DT

during the first three weeks (tumor blood vessel formation phase) was shorter than that during weeks three to seven (blood vessel stabilization phase). The reason may be that the tumor growth relies on the new blood vessels to supply nutrition. Angiogenesis is stronger in the tumor blood vessel formation phase.

Docetaxel, a semisynthetic taxane for the treatment of lung cancer, acts by binding to the β-subunit of tubulin and promotes stabilization of microtubules and causes G2/M cell cycle arrest [26]. It significantly induces of apoptosis [27] and antiangiogenic activity [28,29]. Our study confirmed that the tumor in group C had lower apoptosis and grew well after incubation by FCM and TUNEL assay. While the tumor was influenced by antitumor drug such as docetaxel, which increased the apoptosis tissues in the VX2 orthotopic lung cancer rabbit model. Therefore, this model is sensitive to taxane chemotherapy drug and may suitable for the evaluation of other antitumor effects of antitumor drugs or novel formulations.

The use of the VX2 orthotopic lung cancer rabbit model has long been hampered by the difficulty of the experimental operation. Our study offers a fast, large-scale and accurate technology to establish this model characterized by less difficulty, mortality, chest seeding and a higher solitary tumor induction rate.

ACKNOWLEDGEMENTS

This study was supported by the National Natural Science Foundation of China (Grant No. 81172097) and the Key Funds of Chongqing Medical University (grant no: XBZD201004).

CONFLICTS OF INTEREST

The authors declare no conflicts of interest.

REFERENCES

1. Stewart BW, Wild CP. World Cancer Report 2014. Lyon: WHO International agency for research on Cancer; 2014.
2. Siegel RL, Miller KD, Jemal A. Cancer statistics, 2016. *CA Cancer J Clin.* 2016;66:7-30.
3. Chen W, Zheng R, Baade PD, Zhang S, Zeng H, Bray F, Jemal A, Yu XQ, He J. Cancer statistics in China, 2015. *CA Cancer J Clin.* 2016;66:115-132.
4. Zhao L, Wei Y, Li W, Liu Y, Wang Y, Zhong X, Yu Y. Solid dispersion and effervescent techniques used to prepare docetaxel liposomes for lung-targeted delivery system: in vitro and in vivo evaluation. *J Drug Target.* 2011;19:171-178.
5. Razi SS, Rehmani S, Li X, Park K, Schwartz GS, Latif MJ, Bhora FY. Antitumor activity of paclitaxel is significantly enhanced by a novel proapoptotic agent in non-small cell lung cancer. *J Surg Res.* 2015;194:622-630.
6. Alibolandi M, Ramezani M, Abnous K, Sadeghi F, Atyabi F, Asouri M, Ahmadi AA, Hadizadeh F. In vitro and in vivo evaluation of therapy targeting epithelial-cell adhesion-molecule aptamers for non-small cell lung cancer. *J Control Release.* 2015;209:88-100.
7. Cho WY, Hong SH, Singh B, Islam MA, Lee S, Lee AY, Gankhuyag N, Kim JE, Yu KN, Kim KH, Park YC, Cho CS, Cho MH. Suppression of tumor growth in lung cancer xenograft model mice by poly(sorbitol-co-PEI)-mediated delivery of osteopontin siRNA. *Eur J Pharm Biopharm.* 2015;94:450-462.
8. Chi L, Na MH, Jung HK, Vadevoo SM, Kim CW, Padmanaban G, Park TI, Park JY, Hwang I, Park KU, Liang F, Lu M, Park J, Kim IS, Lee BH. Enhanced delivery of liposomes to lung tumor through targeting interleukin-4 receptor on both tumor cells and tumor endothelial cells. *J Control Release.* 2015;209:327-336.
9. Liu X, Liu J, Guan Y, Li H, Huang L, Tang H, He J. Establishment of an orthotopic lung cancer model in nude mice and its evaluation by spiral CT. *J Thorac Dis.* 2012;4:141-145.
10. Isobe T, Onn A, Morgensztern D, Jacoby JJ, Wu W, Shintani T, Itasaka S, Shibuya K, Koo PJ, O'Reilly MS, Herbst RS. Evaluation of novel orthotopic nude mouse models for human small-cell lung cancer. *J Thorac Oncol.* 2013;8:140-146.
11. Iochmann S, Lerondel S, Bléchet C, Lavergne M, Pesnel S, Sobilo J, Heuzé-Vourc'h N, Le Pape A, Reverdiau P. Monitoring of tumour progression using bioluminescence imaging and computed tomography scanning in a nude mouse orthotopic model of human small cell lung cancer. *Lung Cancer.* 2012;77:70-76.
12. Shope RE, Hurst EW. Infectious papillomatosis of rabbits: with a note on the histopathology. *J Exp Med.* 1933;58:607-624.
13. Rous P, Beard JW. The progression to carcinoma of virus-induced rabbit papillomas (Shope). *J Exp Med.* 1935;62:523-548.
14. Qin H, Zhang MR, Xie L, Hou Y, Hua Z, Hu M, Wang Z, Wang F. PET imaging of apoptosis in tumor-bearing mice and rabbits after paclitaxel treatment with (18)F(-)Labeled recombinant human His10-annexin V. *Am J Nucl Med Mol Imaging.* 2014;5:27-37.
15. Okuma T, Matsuoka T, Okamura T, Wada Y, Yamamoto A, Oyama Y, Koyama K, Nakamura K, Watanabe Y, Inoue Y. 18F-FDG small-animal PET for monitoring the therapeutic effect of CT-guided radiofrequency ablation on implanted VX2 lung tumors in rabbits. *J Nucl Med.* 2006;47:1351-1358.
16. Zhang Q, Shi B, Liu Z, Zhang M, Zhang W. Preliminary study of CT in combination with MRI perfusion imaging to assess hemodynamic changes during angiogenesis in a rabbit model of lung cancer. *Onco Targets Ther.* 2013;6:685-692.
17. Tu M, Xu L, Wei X, Miao Y. How to establish a solitary and localized VX2 lung cancer rabbit model? A simple and effective intrapulmonary tumor implantation technique. *J Surg Res.* 2009;154:284-292.
18. Xu Yp, Yang M, Pan Dh, Wang Lz, Liu L, Huang P, Shao G. Bioevaluation study of 32P-CP-PLLA particle brachytherapy in a rabbit VX2 lung tumor model. *Appl Radiat Isot.* 2012;70:583-588.
19. Lin LM, Chen YK, Chen CH, Chen YW, Huang AH, Wang WC. VX2-induced rabbit buccal carcinoma: a potential cancer model for human buccal mucosa squamous cell carcinoma. *Oral Oncol.* 2009;45:e196-203.
20. Chen J, White SB, Harris KR, Li W, Yap JW, Kim DH, Lewandowski RJ, Shea LD, Larson AC. Poly(lactide-co-glycolide) microspheres for MRI-monitored delivery of sorafenib in a rabbit VX2 model. *Biomaterials.* 2015;61:299-306.

21. Ranjan A, Jacobs GC, Woods DL, Negussie AH, Partanen A, Yarmolenko PS, Gacchina CE, Sharma KV, Frenkel V, Wood BJ, Dreher MR. Image-guided drug delivery with magnetic resonance guided high intensity focused ultrasound and temperature sensitive liposomes in a rabbit Vx2 tumor model. *J Control Release.* 2012;158:487-494.
22. Anayama T, Nakajima T, Dunne M, Zheng J, Allen C, Driscoll B, Vines D, Keshavjee S, Jaffray D, Yasufuku K. A novel minimally invasive technique to create a rabbit VX2 lung tumor model for nano-sized image contrast and interventional studies. *PLoS One.* 2013;8:e67355.
23. Hanahan D, Folkman J. Patterns and emerging mechanisms of the angiogenic switch during tumorigenesis. *Cell.* 1996;86:353-364.
24. Leader P, Månsson S, Besjakov TEJ. CT and MR imaging of the liver using liver specific contrast media. A comparative study in a tumor model. *Acta Radiol.* 1996;37:242-249.
25. Guan L. Angiogenesis dependent characteristics of tumor observed on rabbit VX2 hepatic carcinoma. *Int J Clin Exp Pathol.* 2015;8:12014-12027.
26. Ringel I, Horwitz SB. Studies with RP 56976 (taxotere): a semisynthetic analogue of taxol. *J Natl Cancer Inst.* 1991;83:288-291.
27. Saloustros E, Georgoulias V. Docetaxel in the treatment of advanced non-small-cell lung cancer. *Expert Rev Anticancer Ther.* 2008;8:1207-1222.
28. Guidolin D, Vacca A, Nussdorfer GG, Ribatti D. A new image analysis method based on topological and fractal parameters to evaluate the angiostatic activity of docetaxel by using the Matrigel assay in vitro. *Microvasc Res.* 2004;67:117-124.
29. Grant DS, Williams TL, Zahaczewsky M, Dicker AP. Comparison of antiangiogenic activities using paclitaxel (taxol) and docetaxel (taxotere). *Int J Cancer.* 2003;104:121-129.